



Dynamics of orbital degrees of freedom probed via isotope $^{121,123}\text{Sb}$ nuclear quadrupole moments in Sb-substituted iron pnictide superconductors

T. Kouchi ^{1,2,*}, K. Yoshinaga,¹ T. Asano,¹ S. Nishioka ^{1,3}, M. Yashima,¹ H. Mukuda,^{1,†} A. Iyo,⁴
T. Kawashima,⁵ and S. Miyasaka⁵

¹Graduate School of Engineering Science, Osaka University, Osaka 560-8531, Japan

²Department of Applied Physics, Tokyo University of Science, Tokyo 125-8585, Japan

³National Institute for Materials Science, Ibaraki 305-0003, Japan

⁴National Institute of Advanced Industrial Science and Technology (AIST), Ibaraki 305-8568, Japan

⁵Graduate School of Science, Osaka University, Osaka 560-0043, Japan



(Received 19 January 2023; revised 31 May 2023; accepted 6 July 2023; published 20 July 2023)

Isotope $^{121,123}\text{Sb}$ nuclei with large electric quadrupole moments are applied to investigate the dynamics of orbital degrees of freedom in Sb-substituted iron(Fe)-based compounds. In the parent compound $\text{LaFe}(\text{As}_{0.6}\text{Sb}_{0.4})\text{O}$, the nuclear-spin relaxation rate $^{121,123}(T_1^{-1})$ at $^{121,123}\text{Sb}$ sites was enhanced at structural transition temperature ($T_s \sim 135$ K), which is higher than Néel temperature ($T_N \sim 125$ K). The isotope ratio $^{123}(T_1^{-1}) / ^{121}(T_1^{-1})$ indicates that the electric quadrupole relaxation due to the dynamical electric field gradient at the Sb site increases significantly toward T_s . It is attributed to the critically enhanced nematic fluctuations of stripe-type arrangement of Fe- $3d_{xz}$ (or $3d_{yz}$) orbitals. In the lightly electron-doped superconducting (SC) compound $\text{LaFe}(\text{As}_{0.7}\text{Sb}_{0.3})(\text{O}_{0.9}\text{F}_{0.1})$, the nematic fluctuations are largely suppressed in comparison with the case of the parent compound; however, it remains a small enhancement below 80 K down to the T_c (~ 20 K). The results indicate that the fluctuations from both the spin and orbital degrees of freedom on the $3d_{xz}$ (or $3d_{yz}$) orbitals can be seen in lightly electron-doped SC state of LaFeAsO-based compounds. We emphasize that isotope $^{121,123}\text{Sb}$ quadrupole moments are a sensitive local probe to identify the dynamics of orbital degrees of freedom in Fe pnictides, which provides an opportunity to discuss the microscopic correlation between the superconductivity and both nematic and spin fluctuations simultaneously, even in the polycrystalline samples.

DOI: [10.1103/PhysRevB.108.014507](https://doi.org/10.1103/PhysRevB.108.014507)

I. INTRODUCTION

Iron (Fe)-based superconductivity $\text{LaFeAs}(\text{O}_{1-y}\text{F}_y)$ ($T_c = 26$ K) appears in the vicinity of stripe-type antiferromagnetic (AFM) order and the structural (nematic) transition from tetragonal (C_4) to orthorhombic (C_2) phases [1,2], and hence the mechanism of the superconductivity has been discussed based on spin fluctuations and nematic (orbital) fluctuations [3–6]. In most Fe-based superconductors composed of hole and electron Fermi surfaces (FSs) of similar size, it has been reported that the low-energy spin fluctuations enhanced toward low temperatures have some correlation with T_c [7–12]. Simultaneously, nematic fluctuations critically enhanced in the superconducting (SC) phase have been reported in single crystals of some Fe-based families, which also revealed a relation with the SC phases [13–16]. In some of the Fe-based SC families, the further high- T_c phases appear again in heavily electron-doped regimes without the nested FSs, such as in $\text{LaFeAsO}_{1-y}(\text{F}/\text{H})_y$ [17,18] and intercalated FeSe [19–21]. In those compounds, the spin fluctuations at low energies are not critically enhanced, in contrast to the former cases in lightly electron-doped SC states. Recently, the analyses in collaboration with the Knight shift measurement enabled us

to extract the characteristic behavior of spin fluctuations with a gap at low energies, which becomes prominent in the re-enhanced high- T_c state of the heavily electron-doped regimes [22], and hence it is proposed to be one of the indispensable factors from the viewpoint of a “spin”-based scenario. On the one hand, due to the lack of large single crystals, the contribution of orbital degrees of freedoms is still unclear in $\text{LaFeAsO}(\text{La}1111)$ -based compounds. The universality and diversity of the SC mechanism should be identified in Fe-based compounds over a wide doping region, including the roles of orbital degrees of freedom in addition to the roles of spin components.

To shed light on the dynamical features of orbital degrees of freedom, we focus on the Sb-substituted Fe pnictides $\text{LaFe}(\text{As,Sb})(\text{O,F})$ in this study [23,24]. In general, the nucleus with $I \geq 1$ possesses not only a magnetic moment but also an electric quadrupole moment (Q). As shown in Table I, the Sb nucleus possesses a relatively large Q that could interact with the possible orbital dynamics through the local fluctuations of the electric field gradient (EFG) at the Sb site. Unfortunately, the earlier ^{75}As ($I=3/2$)-NMR studies in the La1111-based compounds [25–27] could not capture the dynamics of the orbital fluctuations due to the lack of sensitivity. The comparison of isotope $^{121,123}\text{Sb}$ nuclei ($I > 1$) would give us a new insight into nematic fluctuations derived from the degenerate Fe- $3d$ orbitals through the local fluctuations of EFG at the Sb site.

*takayoshi.kouchi@rs.tus.ac.jp

†mukuda.hidekazu.es@osaka-u.ac.jp

TABLE I. Nuclear spin (I), gyromagnetic ratio (γ_n), and quadrupole moment (Q) for nuclei in the La1111-based compounds [32,33,52].

	I	γ_n (MHz/T)	Q (10^{-24} cm 2)
^{57}Fe	1/2	1.3785	–
^{75}As	3/2	7.292	+0.29
^{139}La	7/2	6.0142	+0.2
^{121}Sb	5/2	10.189	–0.543
^{123}Sb	7/2	5.5175	–0.692

In this paper we report an isotope $^{121,123}\text{Sb}$ -NMR investigation on Sb-substituted Fe-pnictides $\text{LaFe}(\text{As}_{1-x}\text{Sb}_x)(\text{O}_{1-y}\text{F}_y)$ in the parent and lightly electron-doped SC (\equiv SC1) phases, detecting the temperature evolution of the low-energy nematic fluctuations of stripe-type arrangement of Fe- $3d_{xz}$ (or $3d_{yz}$) orbitals. Our findings reveal that the isotope $^{121,123}\text{Sb}$ quadrupole moments are a very sensitive nuclear probe to identify the dynamics of orbital degrees of freedom in Fe pnictides, which provides an opportunity to discuss the nematic fluctuations in addition to spin fluctuations systematically in the various types of Fe pnictides.

II. EXPERIMENTAL

Polycrystalline samples of $\text{LaFe}(\text{As}_{1-x}\text{Sb}_x)(\text{O}_{1-y}\text{F}_y)$ were synthesized using a solid-state reaction method [24]. Powder x-ray diffraction (XRD) measurement indicates that the lattice parameters monotonically change with x and y , as reported in Ref. [24]. The T_c values were determined from an onset of zero resistivity and diamagnetic response in dc susceptibility measurement [24]. NMR measurements are performed at $^{121,123}\text{Sb}$, ^{75}As , and ^{139}La sites for the coarse-powder samples of Sb-substituted parent $\text{LaFe}(\text{As}_{0.6}\text{Sb}_{0.4})\text{O}$ (denoted as “F0Sb40” hereafter) and lightly electron-doped SC compounds $\text{LaFe}(\text{As}_{0.7}\text{Sb}_{0.3})(\text{O}_{0.9}\text{F}_{0.1})$ (“F10Sb30,” $T_c = 20$ K) and $\text{LaFeAs}(\text{O}_{0.9}\text{F}_{0.1})$ (“F10Sb0,” $T_c = 28$ K) as shown in Fig. 1. The nuclear-spin-lattice relaxation rates ($1/T_1$) were measured at the resonance peak corresponding to the external field perpendicular to the c axis denoted by the arrows in Figs. 2(a)–2(c), determined by fitting a recovery curve for nuclear magnetization to the multiple exponential functions: $m(t) = 0.1 \exp(-t/T_1) + 0.9 \exp(-6t/T_1)$ for $I = 3/2$, $m(t) = 0.028 \exp(-t/T_1) + 0.178 \exp(-6t/T_1) + 0.794 \exp(-15t/T_1)$ for $I = 5/2$, and $m(t) = 0.012 \exp(-t/T_1) + 0.068 \exp(-6t/T_1) + 0.206 \exp(-15t/T_1) + 0.714 \exp(-28t/T_1)$ for $I = 7/2$ [28].

III. RESULTS AND DISCUSSION

A. Parent compound $\text{LaFe}(\text{As}_{0.6}\text{Sb}_{0.4})\text{O}$ (“F0Sb40”)

Figure 2(a) shows the temperature (T) dependence of the ^{121}Sb -NMR spectra for the parent “F0Sb40.” The typical powder pattern spectra are observed at high temperatures. The spectra become broader upon cooling below 125 K, which is also seen in ^{75}As - and ^{139}La -NMR spectra, as shown in Figs. 2(b) and 2(c), respectively. As shown by the solid curves

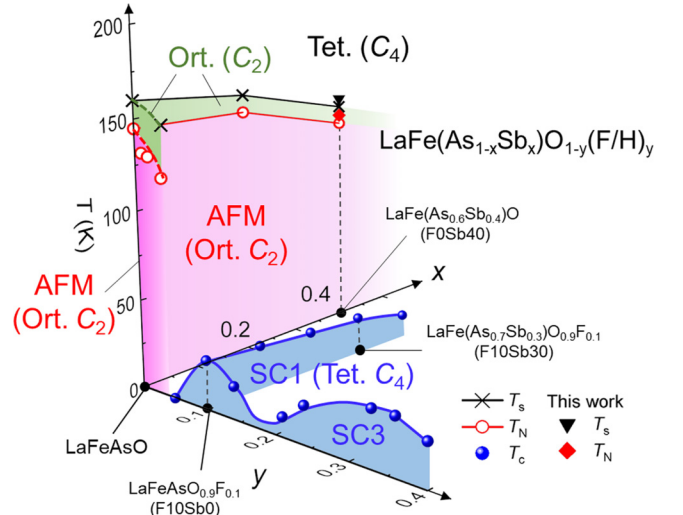


FIG. 1. Phase diagram of $\text{LaFe}(\text{As}_{1-x}\text{Sb}_x)\text{O}_{1-y}(\text{F}/\text{H})_y$, obtained from Refs. [17,23,24]. The present NMR studies are performed on the parent $\text{LaFe}(\text{As}_{0.6}\text{Sb}_{0.4})\text{O}$ (denoted as “F0Sb40”), and the lightly electron-doped SC1 compounds $\text{LaFe}(\text{As}_{0.7}\text{Sb}_{0.3})(\text{O}_{0.9}\text{F}_{0.1})$ (“F10Sb30,” $T_c = 20$ K), together with the Sb-free $\text{LaFeAs}(\text{O}_{0.9}\text{F}_{0.1})$ (“F10Sb0,” $T_c = 28$ K) for comparison.

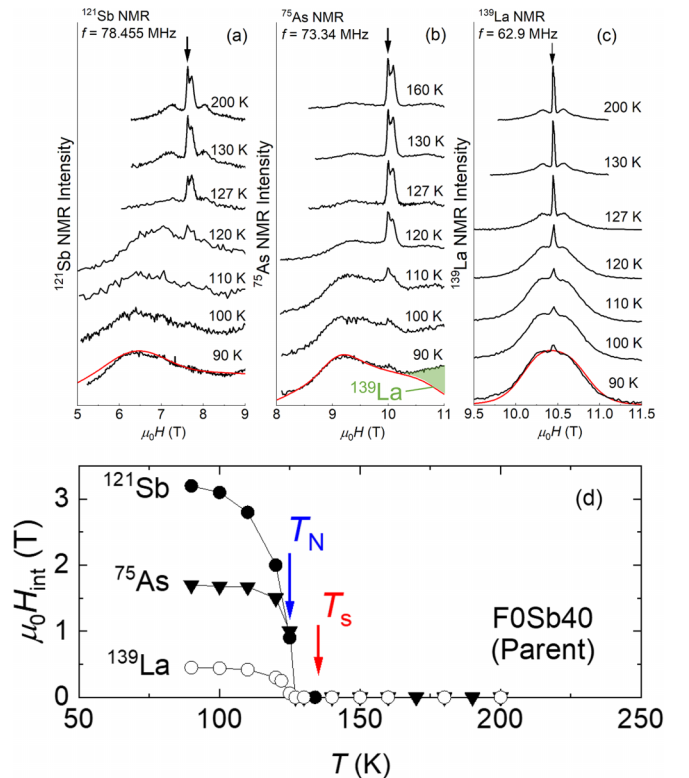


FIG. 2. T dependence of (a) ^{121}Sb , (b) ^{75}As , and (c) ^{139}La -NMR spectra for the parent “F0Sb40.” The arrows denote the resonance peak corresponding to $H \perp c$. Solid curves at 90 K ($\ll T_N$) are simulations obtained by assuming H_{int} and ν_Q at each site (see text). (d) T dependence of H_{int} for all nuclear sites indicates the anomaly due to the static AFM order below $T_N \sim 125$ K for F0Sb40, which is lower than the structural transition at $T_S \sim 135$ K.

in these figures, the NMR spectra at 90 K can be reproduced by the parameters of the internal field (H_{int}) and nuclear quadrupole resonance (NQR) frequency (ν_Q) for each nuclear site: These are $^{121}H_{\text{int}} \sim 3.2$ T and $^{121}\nu_Q \sim 10.5$ MHz for ^{121}Sb site, $^{75}H_{\text{int}} \sim 1.6$ T and $^{75}\nu_Q \sim 11.5$ MHz for ^{75}As site, and $^{139}H_{\text{int}} \sim 0.34$ T and $^{139}\nu_Q \sim 1.8$ MHz for ^{139}La site. These H_{int} are comparable to those of typical parent iron pnictides in the stripe AFM order, such as BaFe_2As_2 [29] and LaFeAsO [26]. The H_{int} for these nuclear sites exhibit a rapid increase below 125 K, as summarized in Fig. 2(d), indicating that the AFM order develops below Néel temperature $T_N \sim 125$ K homogeneously over the crystals. The values of H_{int} depend on that of the hyperfine-coupling constant (A_{hf}) at these nuclear sites, since it is given by the relation $^iH_{\text{int}} = A_{\text{hf}}M_{\text{AFM}}$, where M_{AFM} is an AFM moment at the Fe site. By using $^{75}A_{\text{hf}} \sim 2.0\text{--}2.5T/\mu_B$, estimated at the As site of La1111 [27,30], the M_{AFM} can be estimated to be $0.64\text{--}0.80 \mu_B$, which is comparable to the values observed for the parent LaFeAsO [31]. We note that the $^{121}H_{\text{int}}$ at Sb site was the largest among the values at these nuclei, owing to the largest magnetic hyperfine coupling between the Sb nucleus and the Fe-3d electrons. This is because the 5p orbitals of the Sb are more extended than those of the As. The relative ratios were evaluated to be $^{121}A_{\text{hf}}/^{75}A_{\text{hf}} \sim 2$ and $^{121}A_{\text{hf}}/^{139}A_{\text{hf}} \sim 9.4$ in this experiment.

Next we focus on the electronic states through the measurement of the nuclear-spin relaxation rate. In the parent F0Sb40, the $1/T_1T$ increases upon cooling and exhibits a peak at $T_N \sim 125$ K due to the static AFM order, as shown in Figs. 3(a)–3(c). Remarkably, the additional peak at 135 K observed for the Sb-NMR probe corresponds to the structural (nematic) transition at T_s that appears slightly above T_N [see Fig. 3(c)]. This suggests that the other relaxation mechanisms are added at the Sb nucleus, which is observed more sensitively than at the other nuclei. In general, when the nucleus possesses an electric quadrupole moment (Q), the observed relaxation rates are composed of the magnetic contribution $(1/T_1T)_M$ and an electric one $(1/T_1T)_Q$. The $(1/T_1T)_M$ is generally described as

$$\left(\frac{1}{T_1T}\right)_M \propto \gamma_n^2 \lim_{\omega \rightarrow 0} \sum_{\vec{q}} A_{\text{hf}}(\vec{q})^2 \frac{\chi''_m(\vec{q}, \omega)}{\omega}, \quad (1)$$

where $A_{\text{hf}}(\vec{q})$ is the hyperfine-coupling constant at \vec{q} , and $\chi''_m(\vec{q}, \omega)$ is dynamical spin susceptibility at wave vector \vec{q} and energy ω [32,33]. In usual metals and alloys, the magnetic part $(1/T_1T)_M$ is predominant through the large Fermi-contact interaction with electron spins on conduction bands, resulting in the electric relaxation part $(1/T_1T)_Q$ being negligible. However, in the case of Fe pnictides, the electric part $(1/T_1T)_Q$ can be enhanced by the fluctuations of EFG between the C_2 and C_4 symmetry. According to previous studies [34–39], it could be expressed by

$$\left(\frac{1}{T_1T}\right)_Q \propto f(I)(eQ)^2 \lim_{\omega \rightarrow 0} \sum_{\vec{q}} \frac{\chi''_{\text{nem}}(\vec{q}, \omega)}{\omega}, \quad (2)$$

where the $f(I)$ is $(2I+3)/(I^2(2I-1))$, and χ''_{nem} is the dynamical nematic susceptibility [34]. Thus if only magnetic relaxation mechanism is dominant, the relaxation rate

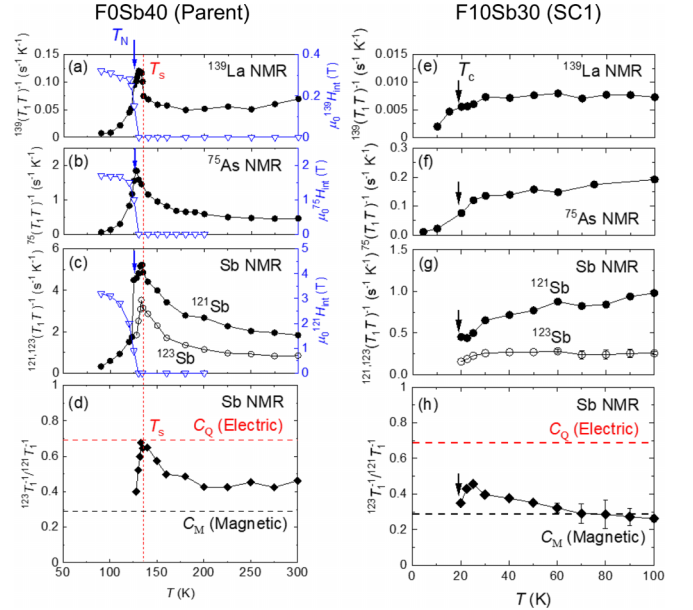


FIG. 3. T dependence of $1/T_1T$ and H_{int} at (a) La, (b) As, and (c) Sb sites of the parent (F0Sb40). The $1/T_1T$ s at three nuclear sites increases significantly upon cooling toward $T_N \sim 125$ K, while only $1/T_1T$ at the Sb site shows an additional anomaly at $T_s \sim 135$ K. (d) T dependence of the ratio $^{123}(T_1^{-1})/^{121}(T_1^{-1})$ at isotopic Sb sites for F0Sb40, indicating that the electric relaxation becomes dominant around T_s due to the critical slowing down of the orbital fluctuations. As for the lightly doped SC sample (F10Sb30), the results of $1/T_1T$ for (e) La, (f) As, and (g) Sb sites are shown. (h) Their isotope ratio $^{123}(T_1^{-1})/^{121}(T_1^{-1})$ suggests a moderate enhancement due to the nematic fluctuations below 80 K in the lightly doped SC1 phase.

should be proportional to the square of γ_n , resulting in an isotopic ratio of the relaxation rate $(^{123}T_1^{-1})_M/(^{121}T_1^{-1})_M$ approaching $(^{123}\gamma_n/^{121}\gamma_n)^2 = 0.293 (\equiv C_M)$. In contrast, if only the electric relaxation mechanism is dominant, the isotopic ratio $(^{123}T_1^{-1})_Q/(^{121}T_1^{-1})_Q$ is expected to be $f(7/2)(^{123}Q^2)/f(5/2)(^{121}Q^2) = 0.691 (\equiv C_Q)$.

Figure 3(d) shows the T dependence of $^{123}(T_1^{-1})/^{121}(T_1^{-1})$. Remarkably, it is close to the value of C_Q at around T_s , indicating that the electric relaxation process at the Sb site is critically enhanced toward T_s . It is obviously attributed to the critical slowing down for the stripe-type alignment of the Fe-3d_{xz} (or 3d_{yz}) orbital at T_s from the tetragonal (C_4) to the orthorhombic (C_2) phase. The fluctuations of in-plane anisotropy in EFG are induced by the dynamics of the local charge distribution at Sb-5p_{x,y} orbitals that hybridize with Fe-3d_{xz,yz} orbitals, as discussed in the lightly doped 122-based Fe pnictides [34]. We also note that at high temperatures this ratio stays at the intermediate value (~ 0.45) between C_M and C_Q , indicating that the magnetic and electric relaxation components are almost comparable, even above T_s . It suggests that the nematic fluctuations between the C_4 and C_2 symmetries remain even in the C_4 phase well above T_s .

Next we attempt to extract the electric relaxation component to estimate the outline of T evolution of nematic fluctuations. Here we made the approximation of simple addition of the relaxation rates of the two channels, expressed as

$i(1/T_1T) \equiv iR = i(1/T_1T)_M + i(1/T_1T)_Q$ ($i = 121, 123$). In this analysis we note that when the $(1/T_1T)_Q$ term is more enhanced, the functional form of the relaxation is a complex mixture of terms arising from both magnetic and quadrupole interaction channels [35,36]. We attempt to use the same functional form of the relaxation shown in Sec. II, which will give us information on the outline of T -evolution of nematic fluctuations over some ambiguity in the absolute value of T_1 . First we consider that the orbital fluctuations also contribute to the magnetic relaxation very rarely through the possible terms, $(1/T_1T)_M^{\text{orb}} \propto \gamma_n^2 \lim_{\omega \rightarrow 0} \sum_{\vec{q}} (A_L)^2 \chi''_{\text{nem}}(\vec{q}, \omega) / \omega$ [37,38], where the A_L is the magnetic hyperfine-coupling constant that appears due to the coupling with χ_{nem} in the case of Fe pnictides. It will cause the magnetic relaxation; however, it may be negligibly smaller than the component of spin fluctuations [Eq. (1)], since the ratio $^{123}(T_1^{-1}) / ^{121}(T_1^{-1})$ is close to C_Q at T_s , where the χ_{nem} is largely enhanced. Therefore it is assumed that the magnetic (spin) and electric (orbital) relaxation components may be handled independently in the relaxation process. Thus the observed ratio $^{123}(T_1^{-1}) / ^{121}(T_1^{-1})$ is given by

$$\frac{^{123}(T_1^{-1})}{^{121}(T_1^{-1})} = \frac{^{123}R}{^{121}R} \sim \frac{^{123}R_M + ^{123}R_Q}{^{121}R_M + ^{121}R_Q}. \quad (3)$$

Hence $^{121}R_Q [\equiv ^{121}(1/T_1T)_Q]$ is tentatively extracted from the relation expressed as

$$^{121}R_Q \sim ^{121}R \left[1 - \frac{1 - C_Q(^{121}R/^{123}R)}{(C_M - C_Q)(^{121}R/^{123}R)} \right], \quad (4)$$

where $C_M = 0.293$ and $C_Q = 0.691$, and the ratio $(^{123}R/^{121}R)$ is obtained in Fig. 3(d).

Figure 4(a) shows the outline of T dependence of the $^{121}(1/T_1T)_Q$ component. It enables us to estimate the T evolution of the dynamical nematic fluctuations χ''_{nem} at low energies that increases significantly toward T_s . In most of the previous NMR studies using the nuclear quadrupole interaction such as ^{75}As -NMR, the evolution of the *static* nematicity has been discussed, which is evaluated by the static imbalance population between p_x and p_y orbitals at the As (or Se) site for the single crystals such as 122-, 11-, and 111-based compounds [40–43]. The dynamics of nematic fluctuations in these compounds were discussed from the anisotropy of the relaxation rate of their single crystals [44–46]. Less study has focused on the dynamics of nematic states in La1111-based compounds in the earlier ^{75}As -NMR works due to poor sensitivity to the orbital degrees of freedom [25–27]. We note that the novelty of this study is the ability to directly probe the charge fluctuations associated with nematic order, even if it is not limited to a single crystal. The current $^{121,123}\text{Sb}$ nuclear probe possessing the large electric quadrupole moment ($^{121,123}Q$) gives us an opportunity to extract the dynamical feature of the orbital fluctuation sensitively.

B. Lightly electron-doped SC compound LaFe(As_{0.7}Sb_{0.3})(O_{0.9}F_{0.1}) (“F10Sb30”)

Next the same experimental method is applied for the lightly electron-doped SC compound LaFe(As_{0.7}Sb_{0.3})(O_{0.9}F_{0.1}) (“F10Sb30”) ($T_c \sim 20$ K).

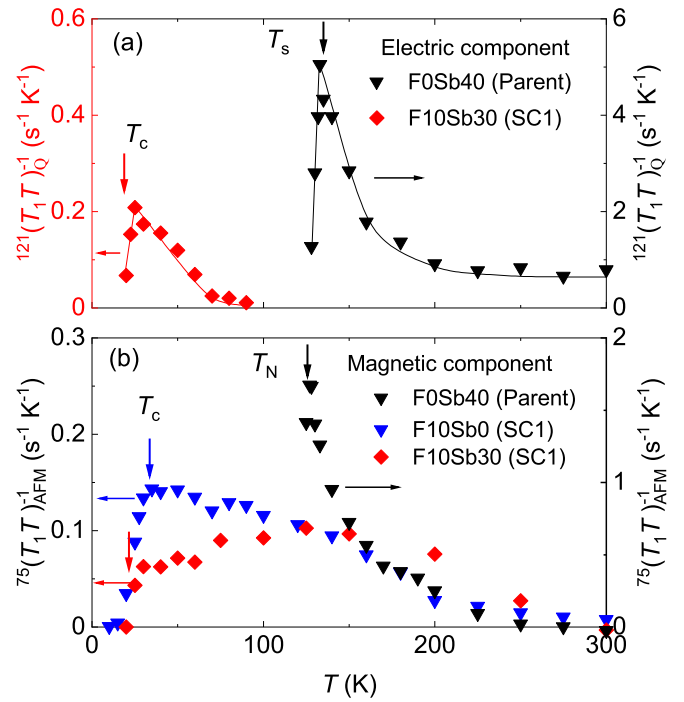


FIG. 4. (a) T dependence of the electric relaxation $^{121}(1/T_1T)_Q$ extracted for the parent (F0Sb40) and lightly electron-doped SC state (F10Sb30), suggesting that the nematic fluctuations observed in the parent are largely suppressed but remain below 80 K in the SC1 phase even in the static C_4 symmetry. (b) Spin fluctuations $^{75}(1/T_1T)_{\text{AFM}}$ deduced for the parent (F0Sb40) and SC1 (F10Sb0 and F10Sb30). In the lightly electron-doped SC1 region, the spin fluctuations are enhanced upon cooling, whereas the suppression of AFMSFs upon cooling becomes characteristic in the Sb-doped sample (F10Sb30) that appears when pnictogen height is high [22].

Figures 3(e)–3(g) show the T dependence of $1/T_1T$ measured at (e) La, (f) As, and (g) Sb sites. There is neither static magnetic order nor the nematic order, i.e., the tetragonal(C_4) structure is stable in the whole T range, and hence the $1/T_1T$ does not exhibit any peaks. The T dependence of $1/T_1T$ exhibits gradual decreases upon cooling at all the nuclear sites, which is generally seen in lightly electron-doped Fe pnictides, ensuring the lightly electron-doped state. Figure 3(h) shows the T dependence of their isotopic ratio $^{123}(T_1^{-1}) / ^{121}(T_1^{-1})$ at the $^{121,123}\text{Sb}$ site. We found that it is close to the magnetic ratio ($C_M = 0.293$) at high T , but it approaches gradually upon cooling toward the electric ratio ($C_Q = 0.691$), indicating that the electrical relaxation due to the dynamical nematic fluctuations between C_4 and C_2 symmetries is not negligible below 80 K for the lightly electron-doped SC1 states, although it keeps the static C_4 symmetry from a macroscopic point of view. Note that the scales of $^{121}(1/T_1T)_Q$ for parent (F0Sb40) and SC1 (F10Sb30) are about 10 times different, as seen in the right and left axes in Fig. 4(a), respectively. This large difference seems to be remarkable beyond some ambiguity in the absolute value of T_1 in this analysis. In the previous ^{75}As -NMR measurement of BaFe₂(As_{0.67}P_{0.33})₂ ($T_c = 31$ K), it was revealed that the nematic fluctuations were also enhanced toward low

T in the superconducting phase with C_4 symmetry by comparing the relaxation rate between $^{31}\text{P}(I = 1/2)$ and $^{75}\text{As}(I = 3/2)$ nucleus [34]. The dynamics of nematic states seen in $\text{BaFe}_2(\text{As,P})_2$ [34] can be observed in La1111-based compound (F10Sb30) as well. The nematic fluctuations are enhanced below 100 K in the slightly doped SC phase of both $\text{BaFe}_2(\text{As}_{0.67}\text{P}_{0.33})_2$ ($T_c = 31$ K) and La1111(F10Sb30) ($T_c = 20$ K) within the C_4 symmetry. From these experimental facts, the contribution of nematic fluctuations to SC may not be negligible in the iron pnictides with well-nested or moderately nested FSs.

C. Comparison with AFM spin fluctuations

Next we discuss the AFM spin fluctuations (AFMSFs) probed by ^{75}As -NMR in these compounds, since a number of the previous ^{75}As -NMR reports indicates the observed $^{75}(1/T_1T)$ is generally dominated by magnetic relaxation, that is, $^{75}(1/T_1T)_M$ [7–12,22]. According to these previous works, it is known that the observed $^{75}(1/T_1T)_M$ can be decomposed as $(1/T_1T)_{\text{AFM}} + (1/T_1T)_0$, where the first term $(1/T_1T)_{\text{AFM}}$ represents the component of AFMSFs at finite wave vector $\vec{q} = Q$ in Eq. (1), and the second term $(1/T_1T)_0$ is the component related to the square of the density of states $[N(E_F)]$ that is proportional to the spin part of Knight shift (K_S). The details of this method are described elsewhere [22] and in the Supplemental Material [47].

As a result, Fig. 4(b) shows the estimated $^{75}(1/T_1T)_{\text{AFM}}$ for the parent (F0Sb40) and SC1 (F10Sb0 and F10Sb30). To evaluate the substitution effect of Sb in the SC1 phase, the result of Sb-free compound F10Sb0 ($T_c = 28$ K) in the same doping level is compared. The $^{75}(1/T_1T)_{\text{AFM}}$ in the SC1 (F10Sb0 and F10Sb30) phase increases upon cooling, suggesting the presence of the low-energy spin fluctuations that can be attributed to the well-nested FSs mostly composed of two $d_{xz/yz}$ orbitals [11]. We note that this is not the case of the simple Curie-Weiss type behavior, namely, the $^{75}(1/T_1T)_{\text{AFM}}$ for Sb-substituted F10Sb30 is more suppressed below 100 K than for Sb-free F10Sb0. This behavior is more prominent when the energy level of the d_{xy} orbital band approaches the Fermi level when the pnictogen height becomes high, i.e., Sb content increases [22]. Thus, such small suppression of AFMSFs upon cooling is accounted for by the increment of d_{xy} orbital band contributions in addition to the predominant $d_{xz/yz}$ bands [4,24]. According to the spin-based scenario [3,4], the presence of the low-energy spin fluctuations is one of the important factors for the increment of T_c in the lightly doped SC1 phase, which is consistent with the present experimental fact that it is more significant in Sb-free F10Sb0 ($T_c = 28$ K) than in F10Sb30 ($T_c = 20$ K), since these locate in the lightly doped SC1 region. This is in contrast to the heavily electron-doped SC3 region of La1111 (see Fig. 1), where the lack of spin fluctuations at low energies

is more significant and rather favorable for SC. In other words, the presence of the finite-energy spin fluctuations originating from the predominant d_{xy} band with strong correlations (less contribution from $d_{xz/yz}$ bands) is one of the key factors for the appearance of reemergent SC3 phase in the case of the heavily electron-doped regime [22,48–51].

Consequently, in these experiments we succeeded in the detection of both nematic and spin fluctuations in the SC1 phase, as presented in Figs. 4(a) and 4(b), respectively. This implies that the spin and orbital degrees of freedom are inseparable in nature. To identify the qualitative roles of the effect of the orbital degrees of freedom over a wider doping region as a function of T_c values, the future systematic Sb-NMR measurements are desired from lightly doped SC1 to heavily doped SC3 phases.

IV. SUMMARY

In summary, we succeeded in detecting the dynamics of the stripe-type orbital fluctuations in the Sb-substituted La1111 compounds by the isotope $^{121,123}\text{Sb}$ -NMR probes with the large $^{121,123}\text{Sb}$ quadrupole moments. We revealed that the nematic fluctuations of the stripe-type alignment of Fe- $3d_{xz}$ (or $3d_{yz}$) orbital are critically enhanced toward $T_s \sim 135$ K slightly higher than $T_N \sim 125$ K in the parent (F0Sb40). In the lightly electron-doped SC1 phase, such nematic fluctuations are largely suppressed, but there remains a small enhancement below 80 K down to the T_c , in spite of keeping the tetragonal (C_4) symmetry. As for the spin degrees of freedom, the AFMSFs are also observed on the SC1 phase due to the well-nested FSs derived mainly from $3d_{xz/yz}$ orbitals, with some additional contribution from the $3d_{xy}$ orbital, especially when the pnictogen height is large. The results suggest that both the spin and orbital degrees of freedom on the $3d_{xz/yz}$ orbitals can be seen in the lightly electron-doped SC1 phase, implying that they are not completely separated in the Fe pnictide superconductors. The future systematic NMR measurements over a wide electron doping region will give us a qualitative evaluation of the effect of the orbital degrees of freedom from SC1 to heavily electron-doped SC3. We emphasize here that the present isotope Sb-NMR provides an approach to investigate the correlation between orbital and spin fluctuations and the SC state in La1111 systems systematically, even in polycrystalline samples.

ACKNOWLEDGMENTS

One of the authors (T.K.) is supported by a JSPS fellowship (Grant No. 21J14053). This work was supported by JSPS KAKENHI (Grant No. 18K18734), the Iketani Science and Technology Foundation, Izumi Science and Technology Foundation, the Casio Science Promotion Foundation, and Takahashi Industrial and Economic Research Foundation.

[1] Y. Kamihara, T. Watanabe, M. Hirano, and H. Hosono, *J. Am. Chem. Soc.* **130**, 3296 (2008).

[2] H. Luetkens, H.-H. Klaus, M. Kraken, F. J. Litterst, T. Dellmann, R. Klingeler, C. Hess, R. Khasanov, A. Amato,

- C. Baines, M. Kosmala, O. J. Schumann, M. Braden, J. Hamann-Borrero, N. Leps, A. Kondrat, G. Behr, J. Werner, and B. Bühner, *Nat. Mater.* **8**, 305 (2009).
- [3] I. I. Mazin, D. J. Singh, M. D. Johannes, and M. H. Du, *Phys. Rev. Lett.* **101**, 057003 (2008).
- [4] K. Kuroki, S. Onari, R. Arita, H. Usui, Y. Tanaka, H. Kontani, and H. Aoki, *Phys. Rev. Lett.* **101**, 087004 (2008).
- [5] H. Kontani and S. Onari, *Phys. Rev. Lett.* **104**, 157001 (2010).
- [6] S. Onari and H. Kontani, *Phys. Rev. Lett.* **109**, 137001 (2012).
- [7] T. Imai, K. Ahilan, F. L. Ning, T. M. McQueen, and R. J. Cava, *Phys. Rev. Lett.* **102**, 177005 (2009).
- [8] F. L. Ning, K. Ahilan, T. Imai, A. S. Sefat, M. A. McGuire, B. C. Sales, D. Mandrus, P. Cheng, B. Shen, and H.-H. Wen, *Phys. Rev. Lett.* **104**, 037001 (2010).
- [9] Y. Nakai, T. Iye, S. Kitagawa, K. Ishida, H. Ikeda, S. Kasahara, H. Shishido, T. Shibauchi, Y. Matsuda, and T. Terashima, *Phys. Rev. Lett.* **105**, 107003 (2010).
- [10] T. Oka, Z. Li, S. Kawasaki, G. F. Chen, N. L. Wang, and G. Q. Zheng, *Phys. Rev. Lett.* **108**, 047001 (2012).
- [11] T. Shiotani, H. Mukuda, M. Uekubo, F. Engetsu, M. Yashima, Y. Kitaoka, K. T. Lai, H. Usui, K. Kuroki, S. Miyasaka, and S. Tajima, *J. Phys. Soc. Jpn.* **85**, 053706 (2016).
- [12] P. Wiecek, K. Rana, A. E. Bohmer, Y. Lee, S. L. Bud'ko, P. C. Canfield, and Y. Furukawa, *Phys. Rev. B* **98**, 020507(R) (2018).
- [13] M. Yoshizawa, D. Kimura, T. Chiba, S. Simayi, Y. Nakanishi, K. Kihou, C.-H. Lee, A. Iyo, H. Eisaki, and S. Uchida, *J. Phys. Soc. Jpn.* **81**, 024604 (2012).
- [14] Y. Gallais, R. M. Fernandes, I. Paul, L. Chauviere, Y.-X. Yang, M.-A. Measson, M. Cazayous, A. Sacuto, D. Colson, and A. Forget, *Phys. Rev. Lett.* **111**, 267001 (2013).
- [15] A. E. Bohmer, P. Burger, F. Hardy, T. Wolf, P. Schweiss, R. Fromknecht, M. Reinecker, W. Schranz, and C. Meingast, *Phys. Rev. Lett.* **112**, 047001 (2014).
- [16] S. Hosoi, K. Matsuura, K. Ishida, H. Wang, Y. Mizukami, T. Watashige, S. Kasahara, Y. Matsuda, and T. Shibauchi, *Proc. Natl. Acad. Sci. USA* **113**, 8139 (2016).
- [17] S. Iimura, S. Matsuishi, H. Sato, T. Hanna, Y. Muraba, S. W. Kim, J. E. Kim, M. Takata, and H. Hosono, *Nat. Commun.* **3**, 943 (2012).
- [18] M. Hiraishi, S. Iimura, K. M. Kojima, J. Yamaura, H. Hiraka, K. Ikeda, P. Miao, Y. Ishikawa, S. Torii, M. Miyazaki, I. Yamauchi, A. Koda, K. Ishii, M. Yoshida, J. Mizuki, R. Kadono, R. Kumai, T. Kamiyama, T. Otomo, Y. Murakami, S. Matsuishi, and H. Hosono, *Nat. Phys.* **10**, 300 (2014).
- [19] J. Guo, S. Jin, G. Wang, S. Wang, K. Zhu, T. Zhou, M. He, and X. Chen, *Phys. Rev. B* **82**, 180520(R) (2010).
- [20] Y. Mizuguchi, H. Takeya, Y. Kawasaki, T. Ozaki, S. Tsuda, T. Yamaguchi, and Y. Takano, *Appl. Phys. Lett.* **98**, 042511 (2011).
- [21] A. K. Maziopa, Z. Shermadini, E. Pomjakushina, V. Pomjakushin, M. Bendele, A. Amato, R. Khasanov, H. Luetkens, and K. Conder, *J. Phys.: Condens. Matter* **23**, 052203 (2011).
- [22] T. Kouchi, S. Nishioka, K. Suzuki, M. Yashima, H. Mukuda, T. Kawashima, H. Tsuji, K. Kuroki, S. Miyasaka, and S. Tajima, *Phys. Rev. B* **105**, 144510 (2022).
- [23] S. J. E. Carlsson, F. Levy-Bertrand, C. Marcenat, A. Sulpice, J. Marcus, S. Pairis, T. Klein, M. Nunez-Regueiro, G. Garbarino, T. Hansen, V. Nassif, and P. Toulemonde, *Phys. Rev. B* **84**, 104523 (2011).
- [24] T. Kawashima, S. Miyasaka, H. Tsuji, T. Yamamoto, M. Uekubo, A. Takemori, K. T. Lai, and S. Tajima, *Sci. Rep.* **11**, 10006 (2021).
- [25] Y. Nakai, K. Ishida, Y. Kamihara, M. Hirano, and H. Hosono, *J. Phys. Soc. Jpn.* **77**, 073701 (2008).
- [26] H. Mukuda, N. Terasaki, N. Tamura, H. Kinouchi, M. Yashima, Y. Kitaoka, K. Miyazawa, P. M. Shirage, S. Suzuki, S. Miyasaka, S. Tajima, H. Kito, H. Eisaki, and A. Iyo, *J. Phys. Soc. Jpn.* **78**, 084717 (2009).
- [27] H.-J. Grafe, D. Paar, G. Lang, N. J. Curro, G. Behr, J. Werner, J. Hamann-Borrero, C. Hess, N. Leps, R. Klingeler, and B. Buchner, *Phys. Rev. Lett.* **101**, 047003 (2008).
- [28] A. Narath, *Phys. Rev.* **162**, 320 (1967).
- [29] K. Kitagawa, N. Katayama, K. Ohgushi, M. Yoshida, and M. Takigawa, *J. Phys. Soc. Jpn.* **77**, 114709 (2008).
- [30] F. Sakano, K. Nakamura, T. Kouchi, T. Shiotani, F. Engetsu, K. Suzuki, R. Horikawa, M. Yashima, S. Miyasaka, S. Tajima, A. Iyo, Y.-F. Guo, K. Yamaura, E. Takayama-Muromachi, M. Yogi, and H. Mukuda, *Phys. Rev. B* **100**, 094509 (2019).
- [31] N. Qureshi, Y. Drees, J. Werner, S. Wurmehl, C. Hess, R. Klingeler, B. Buchner, M. T. Fernandez-Diaz, and M. Braden, *Phys. Rev. B* **82**, 184521 (2010).
- [32] A. Abragam, *The Principles of Nuclear Magnetism* (Clarendon, Oxford, 1961).
- [33] C. P. Slichter, *Principles of Magnetic Resonance* (Springer-Verlag, New York/Berlin/Heidelberg, 1992).
- [34] A. P. Dioguardi, T. Kissikov, C. H. Lin, K. R. Shirer, M. M. Lawson, H.-J. Grafe, J.-H. Chu, I. R. Fisher, R. M. Fernandes, and N. J. Curro, *Phys. Rev. Lett.* **116**, 107202 (2016).
- [35] A. Suter, M. Mali, J. Roos, and D. Brinkmann, *J. Phys.: Condens. Matter* **10**, 5977 (1998).
- [36] A. Suter, M. Mali, J. Roos, and D. Brinkmann, *Phys. Rev. Lett.* **84**, 4938 (2000).
- [37] Y. Obata, *J. Phys. Soc. Jpn.* **18**, 1020 (1963).
- [38] Y. Obata, *J. Phys. Soc. Jpn.* **19**, 2348 (1964).
- [39] I. Vinograd, K. R. Shirer, P. Massat, Z. Wang, T. Kissikov, D. Garcia, M. D. Bachmann, M. Horvatic, I. R. Fisher, and N. J. Curro, *npj Quantum Mater.* **7**, 68 (2022).
- [40] S.-H. Baek, D. V. Efremov, J. M. Ok, J. S. Kim, Jeroen van den Brink, and B. Büchner, *Nat. Mater.* **14**, 210 (2015).
- [41] T. Iye, M.-H. Julien, H. Mayaffre, M. Horvatic, C. Berthier, K. Ishida, H. Ikeda, S. Kasahara, T. Shibauchi, and Y. Matsuda, *J. Phys. Soc. Jpn.* **84**, 043705 (2015).
- [42] R. Zhou, L. Y. Xing, X. C. Wang, C. Q. Jin, and G.-q. Zheng, *Phys. Rev. B* **93**, 060502(R) (2016).
- [43] M. Toyoda, Y. Kobayashi, and M. Itoh, *Phys. Rev. B* **97**, 094515 (2018).
- [44] S.-H. Baek, D. Bhoi, W. Nam, B. Lee, D. V. Efremov, B. Büchner, and K. H. Kim, *Nat. Commun.* **9**, 2139 (2018).
- [45] J. Li, B. Lei, D. Zhao, L. P. Nie, D. W. Song, L. X. Zheng, S. J. Li, B. L. Kang, X. G. Luo, T. Wu, and X. H. Chen, *Phys. Rev. X* **10**, 011034 (2020).
- [46] R. Zhou, D. D. Scherer, H. Mayaffre, P. Toulemonde, M. Ma, Y. Li, B. M. Andersen, and M.-H. Julien, *npj Quantum Mater.* **5**, 93 (2020).
- [47] See Supplemental Material at <http://link.aps.org/supplemental/10.1103/PhysRevB.108.014507> for evaluation of the component of the spin fluctuations.
- [48] K. Suzuki, H. Usui, S. Iimura, Y. Sato, S. Matsuishi, H. Hosono, and K. Kuroki, *Phys. Rev. Lett.* **113**, 027002 (2014).

- [49] H. Arai, H. Usui, K. Suzuki, Y. Fuseya, and K. Kuroki, *Phys. Rev. B* **91**, 134511 (2015).
- [50] M. Nakata, D. Ogura, H. Usui, and K. Kuroki, *Phys. Rev. B* **95**, 214509 (2017).
- [51] K. Matsumoto, D. Ogura, and K. Kuroki, *J. Phys. Soc. Jpn.* **89**, 044709 (2020).
- [52] S. Kitagawa, K. Ishida, K. Nakano, T. Yajima, and H. Kageyama, *Phys. Rev. B* **87**, 060510(R) (2013).